phys. stat. sol. (b) **217**, 389 (2000)

Subject classification: 71.15.Mb; 71.15.Pd; 73.20.Hb; S1.3; S5.11

Ab initio Molecular Dynamics Simulations of Reactions at Surfaces

A. GROSS

Physik-Department T30, Technische Universität München, D-85747 Garching, Germany

(Received August 10, 1999)

In general the statistical nature of reactions on surfaces requires the calculation of a very large number of trajectories in order to determine reaction rates. We show that even in massively parallel schemes a sufficient number of trajectories determined from first principles can only be obtained in a approach in which first the potential energy surface (PES) on which the nuclei move is determined and then the dynamical calculations on an appropriate representation of the PES are performed. The PES can nowadays be evaluated in great detail by first-principles methods based on density-functional theory. These electronic structure calculations also allow the investigation of the factors that determine the reactivity of a particular system. We discuss different methods to represent an ab initio PES and present a massively parallel ab initio quantum dynamics approach for the dissociation of hydrogen on metal surfaces.

1. Introduction

Modern ab initio algorithms based on density-functional theory (DFT) allow the determination of the high-dimensional potential energy surface (PES) and the potential gradients for reactions on surfaces at many different configurations [1 to 6]. This is a prerequisite for the ab initio description of reactions due to the complexity of the high-dimensional PES. However, in order to assess the reactivity of a particular system it is necessary to perform calculations of the reaction dynamics [1, 7]. "Traditional" ab initio molecular dynamics methods (AIMD) perform a complete total-energy calculation for each step of the numerical integration of the equations of motion. We will demonstrate that even in massively parallel approaches the number of trajectories that can be calculated by this approach is still well below 100 [8, 9]. It will be shown that there are special cases in which the crucial trajectories originate from a small portion of the relevant phase space so that already from a small number of trajectories useful information can be extracted [9]. But usually this traditional approach does not allow the determination of a sufficient number of trajectories for obtaining reliable reaction rates.

We have therefore proposed a three-step approach for performing ab initio molecular dynamics calculations [10]: First a sufficient number of ab initio total-energy calculations is performed. Then an interpolation scheme is used to fit the ab initio energies and to interpolate between the actual calculated points. And finally the dynamics calculations are performed on this continuous representation of the ab initio PES. In this way easily 100.000 ab initio trajectories can be determined [10] on a workstation. In addition, on such a continuous representation also quantum dynamical calculations can be performed [11 to 13]. Quantum dynamical simulations can actually be less CPU time consuming than classical trajectory calculations for the determination of reaction rates

because the averaging over initial conditions is done automatically in quantum mechanics by choosing the appropriate initial quantum states [10].

In this paper, we will illustrate the three-step approach for the example of dissociation of hydrogen on clean and adsorbate-covered metal surfaces. We will also show that the electronic structure calculations can be used in order to understand the factors determining the reactivity of a particular surface. Furthermore, we will introduce a massively parallel implementation of the very stable coupled-channel scheme [14] we have used to solve the time-independent Schrödinger equation of the interaction of hydrogen with metal surfaces. Because of the use of curvelinear reaction path coordinates this scheme requires the diagonalisation of non-symmetric matrices. Due to the lack of massively parallel public domain diagonalisation schemes for general matrices we implemented a second order pertubation diagonalisation scheme. We will present results concerning the performance and scaling properties of this ab initio quantum dynamics scheme.

2. AIMD with the Determination of the Forces "on the Fly"

The first ab initio molecular dynamics study of reactions at surfaces with the determination of the forces "on the fly" was an investigation of the adsorption of Cl_2 on Si(111)-2×1 [8]. Only five trajectories were determined in this study so that the information about the reaction dynamics gained from this study was rather limited.

Here we focus on a more recent example, the desorption of hydrogen from Si(100). The interaction of hydrogen with silicon surfaces is of strong technological relevance. On the one hand, hydrogen is used to passivate silicon surfaces, on the other hand, hydrogen desorption from silicon is an important step in the chemical vapor deposition (CVD) growth of silicon substrates.It is a well-studied system [1, 15], but still it is discussed very controversely, as far as experiment [16 to 18] as well as theory is concerned [9, 19]. One of the debated issues is the role of the surface rearrangement of the silicon substrate degrees of freedom upon the adsorption and desorption of hydrogen.

In Fig. 1 this surface rearrangement is illustrated for the Si(100) surface. While at the hydrogen covered monohydride surface the outermost silicon atoms form symmetric dimers (Fig. 1a), at the clean surface these dimers are buckled (Fig. 1c). Consequently,

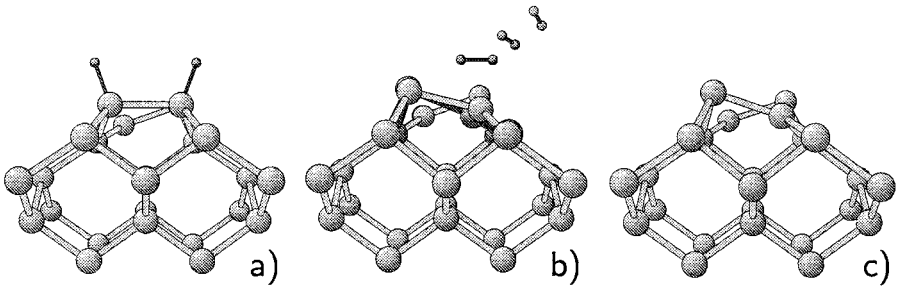

Fig. 1. a) Hydrogen covered Si(100) surface (monohydride). b) Snapshots of a trajectory of D_2 desorbing from Si(100) starting at the transition state with the Si atoms initially at rest [9]. The dark Si atoms correspond to the Si positions after the desorption event. c) Clean anti-buckled Si(100) surface [9]

the silicon surface atoms participate in the hydrogen adsorption and desorption process. In order to investigate the energy redistribution among the different hydrogen and silicon substrate degrees of freedom upon the desorption of hydrogen from Si(100) we have performed AIMD calculations [9] using the Generalized Gradient Approximation (GGA) for the treatment of the exchange and correlation effects. The forces necessary to integrate the equations of motion were determined by DFT calculations for every step of the numerical integration routine. The electronic wave functions were expanded in a plane-wave basis set with a cutoff of 40 Ry, and we used two *k*-points in the irreducible part of the Brillouin zone. The calculations had been performed using the massively parallel version of the fhi96md code [20]. We chose a time step of 1.2 fs in the numerical integration of the motion which took about 20 min on 64 nodes of a Cray T3D. In total 40 trajectories of D_2 desorbing form Si(100) have been determined in that fashion. Fig. 1b shows some snapshots of such a trajectory. It illustrates how the silicon atom beneath the desorbing D_2 molecule relaxes after the desorption thereby gaining a kinetic energy of about 0.1 eV.

However, the number of 40 trajectories is usually much too small to determine any reaction probabilities. Only in certain cases as the hydrogen desorption from Si(100) where the crucial trajectories originate from a small portion of the relevant phase space one can still get reasonable information out of a small number of trajectories. The results of the AIMD calculations were in good quantitative agreement with the experiment [9], except for the experimentally observed low kinetic energy of desorbing D_2 molecules [16] which is still highly debated [1].

Usually the calculation of reaction probabilities requires the determination of the order of 10^3 to 10^6 trajectories or a quantum dynamical scheme. Ab initio molecular dynamics simulations with the determination of the forces "on the fly" are still far away from fulfilling this requirement, as was just shown. The calculation of ab initio reaction probabilities can only be achieved by a three-step approach which will be presented in the next section.

3. Three-Step Approach to AIMD

3.1 Determination of the ab initio potential energy surface

The first step in the general scheme for determining the ab initio dynamics of reactions at surfaces is represented in Fig. 2, namely the determination of the ab initio PES by density-functional theory calculations [4]. It has turned out that it is crucial to treat the exchange–correlation effects in the DFT calculations within the generalized gradient approximation (GGA) in order to obtain realistic barrier heights for the hydrogen dissociation on surfaces [2]. For the hydrogen dissociation on close-packed metal surfaces usually the surface rearrangement upon hydrogen adsorption is negligible. Still total energies for several hundred different configurations have to be determined in order to gain sufficient information about the PES as a function of the molecular coordinates. For the PES of the interaction of hydrogen with Pd(100) total energies of approximately 250 different configurations were calculated. In a later study energies for more than 750 different configurations were computed [21] which resulted in a better agreement of the dynamical calculations based on these ab initio input points with the experiment [7].

As Fig. 2 shows, the PES of the interaction of hydrogen with Pd(100) has non-activated paths towards dissociative adsorption and no molecular adsorption well. However, the majority of pathways towards dissociative adsorption has in fact energy barriers with a rather broad distribution of heights and positions, i.e. the PES is strongly anisotropic and corrugated. That is the reason why so many DFT calculations are needed.

The DFT-GGA calculations can also be used in order to understand the electronic factors that determine the reactivity of a surface [22 to 24]. We will illustrate this for the case of the H_2 dissociation at the (2×2) sulfur-covered Pd(100) surface. The pre-

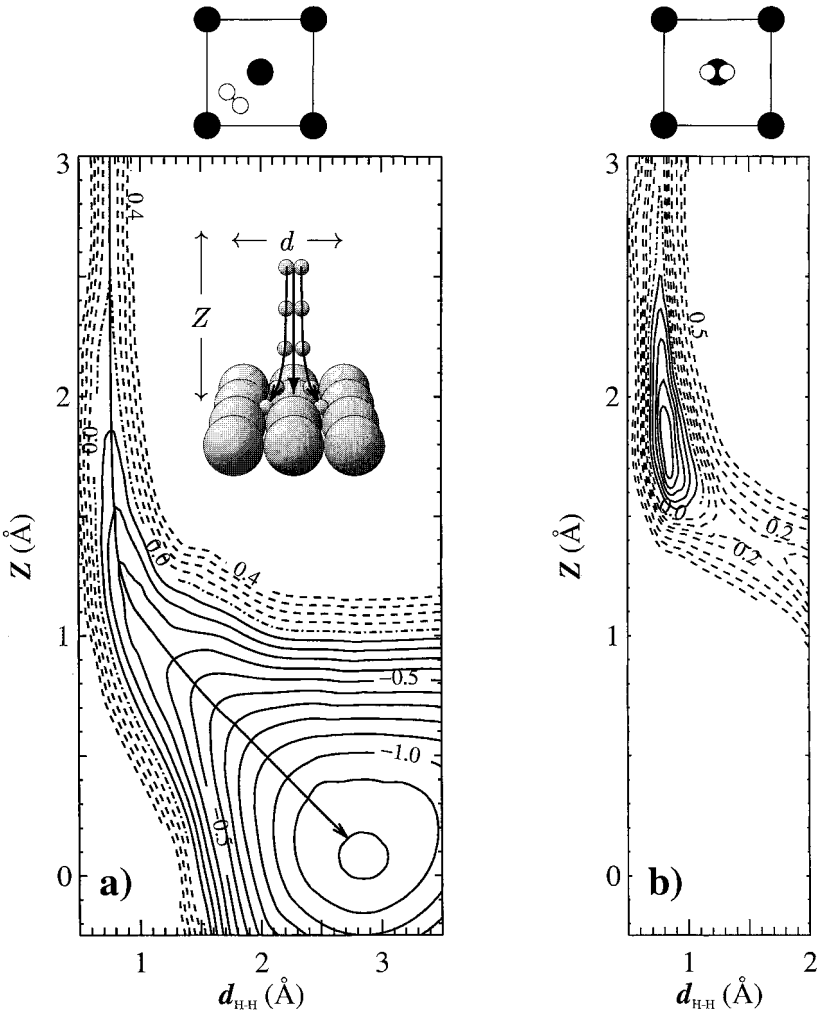

Fig. 2. Contour plots of the PES along two two-dimensional cuts through the six-dimensional coordinate space of H_2/Pd (100), so-called elbow plots, determined by GGA calculations [4]. The coordinates in the figure are the H_2 center-of-mass distance from the surface Z and the H–H interatomic distance d. The lateral H_2 center-of-mass coordinates in the surface unit cell and the orientation of the molecular axis are depicted above the elbow plots. Energies are in eV per H_2 molecule. The contour spacing in a) is 0.1 eV, while it is 0.05 eV in b)

sence of an adsorbate on a surface can profoundly change the surface reactivity. An understanding of the underlying mechanisms and their consequences on the reaction rates is of decisive importance for, e.g., designing better catalysts. Sulfur is known to reduce the reactivity of the Pt-based car exhaust catalyst, hence it is important to analyse the reasons for this so-called poisoning. Hydrogen adsorption on Pd(100) can be used as a model system because on Pd(100) sulfur preadsorption also leads to the poisoning, i.e., the hydrogen dissociation is no longer non-activated as on the clean Pd(100) surface.

This is demonstrated in Fig. 3 where we have collected four elbow plots of the hydrogen dissociation on the (2×2) sulfur covered Pd(100) surface determined by GGA-DFT calculations [22, 24]. These calculations show that hydrogen dissociation on sulfur-covered Pd(100) is still exothermic, however, the dissociation is hindered by the formation of energy barriers in the entrance channel of the PES. The minimum barrier, which is shown in Fig. 3a, has a height of 0.1 eV and corresponds to a configuration in which the H_2 center of mass is located above the fourfold hollow site. This is the site which is farthest away from the sulfur atoms in the surface unit cell. The closer the hydrogen molecule is to the sulfur atoms on the surface, the larger the barrier towards dissociative adsorption becomes. Directly over the sulfur atoms the barrier has a height of 2.5 eV. To our knowledge, this is the most corrugated surface for dissociative adsorption studied so far by ab initio calculations.

In order to understand the origins for the formation of this huge variety in the barrier heights, we have analysed the density of states (DOS) for the H_2 molecule in these different geometries. The information provided by the density of states alone is often not sufficient to assess the reactivity of a particular system. It is also essential to know the character of the occupied and unoccupied states. For the dissociation the occupation of the bonding σ_g and the anti-bonding σ_u^* H_2 molecular levels *and* of the bonding and anti-bonding states with respect to the surface–molecule interaction are of particular importance. We will see that the barrier distribution of the H_2 dissociation over (2×2)S/Pd(100) can be understood by a combination of direct and indirect electronic effects.

The DOS for the situation without any interaction between molecule and surface, i.e, when the H_2 molecule is still far away from the surface, is shown in Fig. 4a. However, the electronic states of the adsorbed sulfur, in particular the p orbitals, are strongly hybridized with the Pd d states. The d band at the surface Pd atoms is broadened and shifted down somewhat with respect to the clean surface due to the interaction with the S atoms [24]. The intense peak in the hydrogen DOS at -4.8 eV which corresponds to the σ_g state is degenerate with the sulfur related bonding state at -4.8 eV. This degeneracy, however, is accidental, as will become evident immediately.

When the molecule comes closer to the surface, the σ_g state starts interacting with the Pd d band. At the minimum barrier position of Fig. 3a the σ_g state has shifted down to -7.1 eV, as Fig. 4b shows. On the other hand, the sulfur state at -4.8 eV remains almost unchanged. This indicates that there is no direct interaction between hydrogen and sulfur. Furthermore, we find a broad distribution of hydrogen states with a small, but still significant weight below the Fermi level. These are states of mainly H_2-surface antibonding character [22, 24] which become populated due to the sulfur induced downshift of the Pd d band. These H_2-surface antibonding states lead to a repulsive interaction and thus to the building up of the barriers in the entrance channel of the PES [24]. It is therefore an indirect interaction between sulfur and hydrogen that is responsible for

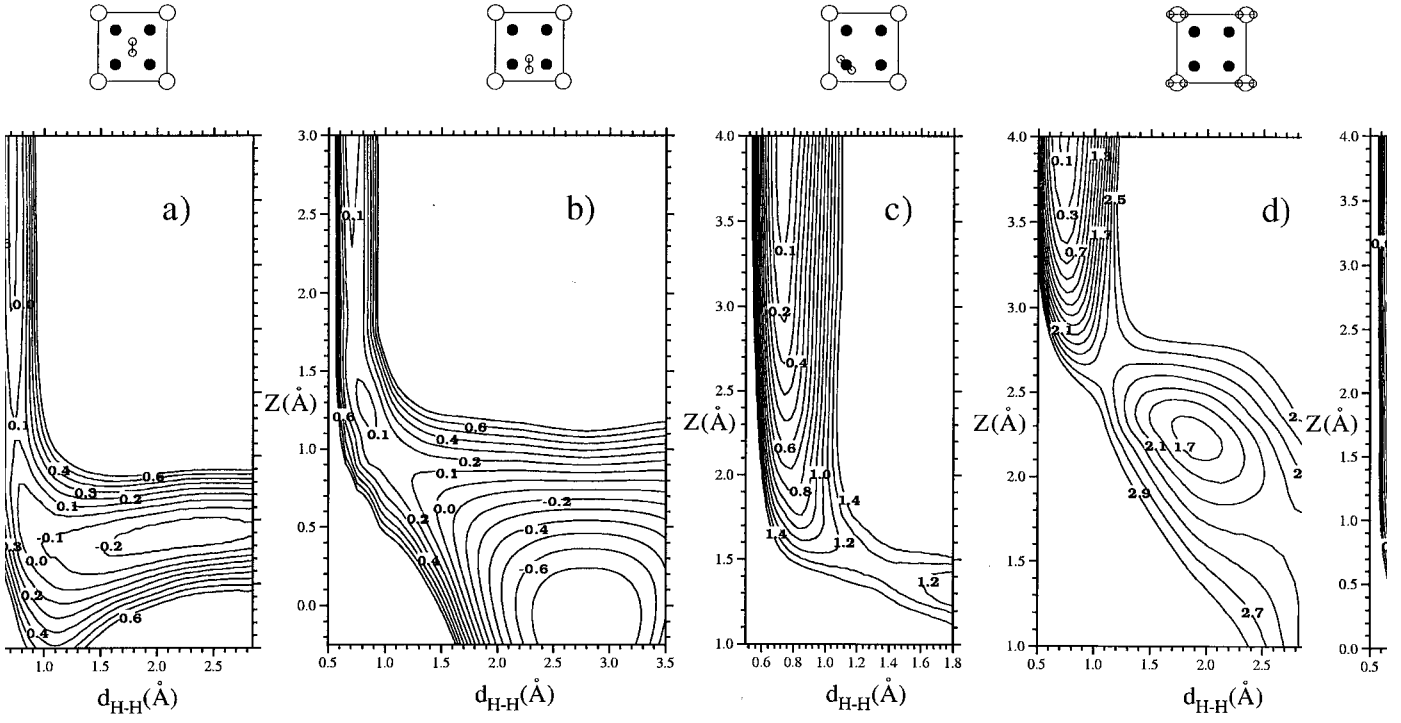

Fig. 3. Cuts through the six-dimensional potential energy surface (PES) of H_2 dissociation over (2×2)S/Pd(100) at four different sites with the molecular axis parallel to the surface: a) at the fourfold hollow site; b) at the bridge site between two Pd atoms; c) on top of a Pd atom; d) on top of a S atom. The energy contours, given in eV per molecule, are displayed as a function of the H–H distance, d_{H-H}, and the height Z of the center-of-mass of H_2 above the topmost Pd layer. The geometry of each dissociation pathway is indicated in the panel above the contour plots. The large open circles are the sulfur atoms, the large filled circles are the palladium atoms (from [22])

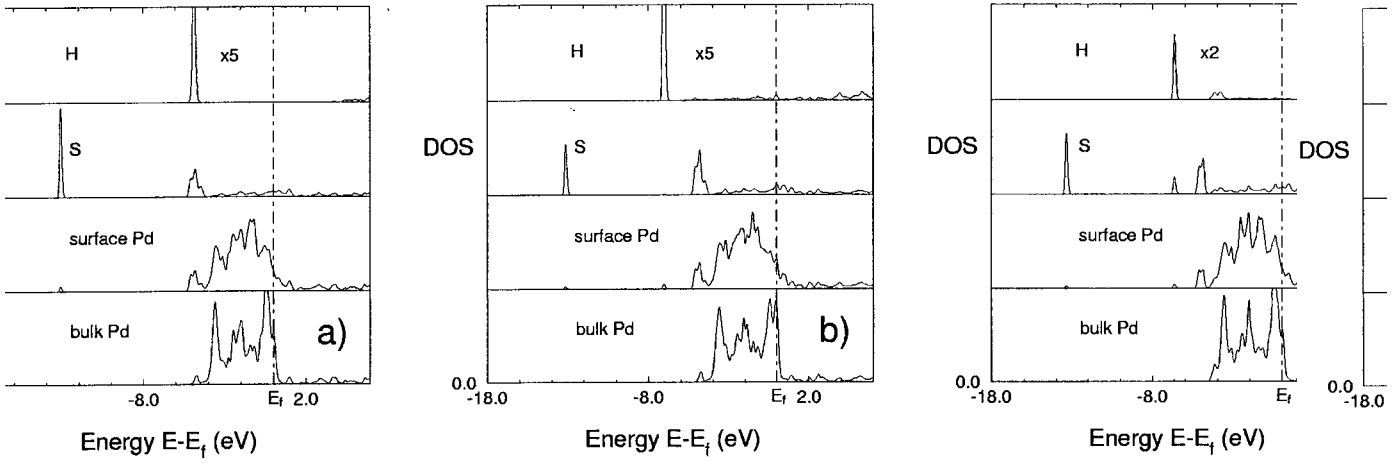

Fig. 4. Density of states (DOS) for a H_2 molecule situated at a) $(Z, d_{H-H}) = (4.03\ \text{Å}, 0.75\ \text{Å})$ and b) $(Z, d_{H-H}) = (1.61\ \text{Å}, 0.75\ \text{Å})$ above the four-fold hollow site which corresponds to the configuration depicted in Fig. 3a, and for a H_2 molecule situated at c) $(Z, d_{H-H}) = (3.38\ \text{Å}, 0.75\ \text{Å})$ above the sulfur atom which corresponds to the configuration depicted in Fig. 3d. Z and d_{H-H} denote the H_2 center-of-mass distance from the surface and the H–H interatomic distance, respectively. Given is the local DOS at the H atoms, the S adatoms, the surface Pd atoms, and the bulk Pd atoms. The energies are given in eV (from [22])

the barriers at this site. A similar picture explains why for example noble metals are so unreactive for hydrogen dissociation: The low-lying d bands of the noble metals cause a downshift and a substantial occupation of the antibonding H_2-surface states resulting in high barriers for hydrogen dissociation [23].

The situation is entirely different if the molecule approaches the surface above the sulfur atom. This is demonstrated in Fig. 4c. The center of mass of the H_2 molecule is still 3.38 Å above the topmost Pd layer, but already at this distance the hydrogen and the sulfur states strongly couple. The intense peak of the DOS at -4.8 eV has split into a sharp bonding state at -6.6 eV and a narrow anti-bonding state at -4.0 eV. Thus it is a direct interaction of the hydrogen with the sulfur related states that causes the high barriers towards hydrogen dissociation close to the sulfur atoms.

In conclusion, the poisoning of hydrogen dissociation on Pd(100) by adsorbed sulfur is due to a combination of an indirect effect, namely the sulfur-related downshift of the Pd d bands resulting in a larger occupation of H_2-surface antibonding states, with a direct repulsive interaction between H_2 and S close to the sulfur atoms.

3.2 Representing the ab initio PES

The second step in the ab initio dynamics scheme is the interpolation of the ab initio data. For the hydrogen dissociation on close-packed metal surfaces the surface rearrangement due to the impinging hydrogen molecules can be neglected due to the large mass mismatch between hydrogen and the metal substrate. This allows to describe the dissociation dynamics within the six-dimensional PES only considering the molecular degress of freedom. In six dimensions it is still possible to fit the ab initio data to an analytical expression, which has be done successfully for the H_2 dissociation on the clean [10, 11] and sulfur-covered Pd(100) surface [22, 25] and also for the H_2/Cu(100) PES [26]. The case of the H_2/Cu(100) PES, however, shows how difficult still the fitting of a six-dimensional PES is. Due to errors in the fitting an artificial well was introduced in the fitted PES which influenced the results [27].

However, once a reliable analytical fit is found, it is computationally inexpensive to calculate the potential gradients at arbitrary configuration which is needed, e.g, to perform molecular dynamics simulations of reactions. However, it becomes very cumbersome to find an appropriate analytical form if more degrees of freedom like, e.g., surface degrees of freedom, have to be considered. Neural networks offer a very flexible interpolation scheme which has been used for fitting an ab initio PES of chemical reactions [28 to 30]. On the one hand, they require no assumptions about the functional form of the underlying problem, but on the other hand, their parameters have no physical meaning. For that reason a relatively large number of ab initio input points is needed for an accurate description of a whole PES. As an alternative approach, recently a genetic programming scheme has been proposed which searches for both the best functional form and the best set of parameters [31]. This method has so far only been used for three-dimensional potentials so that a proof of its applicability for higher-dimensional problems is still missing.

All the interpolations schemes mentioned so far allow a fast determination of the fitted PES at arbitrary configurations. However, these methods usually require a rather large number of training points in order to reproduce the input PES within a sufficient accuracy. As a rough estimate of the neccessary number of input points, at least three

points are needed for each degree of freedom. Consequently, in six dimensions about 10^3 and in twelve 10^6 ab initio total energy calculations as an input are required. The ab initio determination of such a large number of total energies for molecule–surface systems is still computationally very expensive. Therefore, an intermediate step is needed.

Tight-binding methods with parameters derived from first-principles calculations offer such an intermediate approach. Recently, it has been shown that a non-orthogonal tight-binding total-energy (TBTE) method that so far had successfully been used for material properties [32, 33] can also be applied for fitting an ab initio PES of the dissociation of molecules at surfaces [34]. The parameters of this tight-binding scheme had been fitted to reproduce the ab initio PES for the H_2/Pd(100) system. Figure 5 shows the H_2/Pd(100) PES determined with the tight-binding Hamiltonian. This PES should be compared with the ab initio results of Fig. 2. The comparison reveals that indeed the tight-binding method is able to accurately reproduce an ab initio PES. Moreover, due

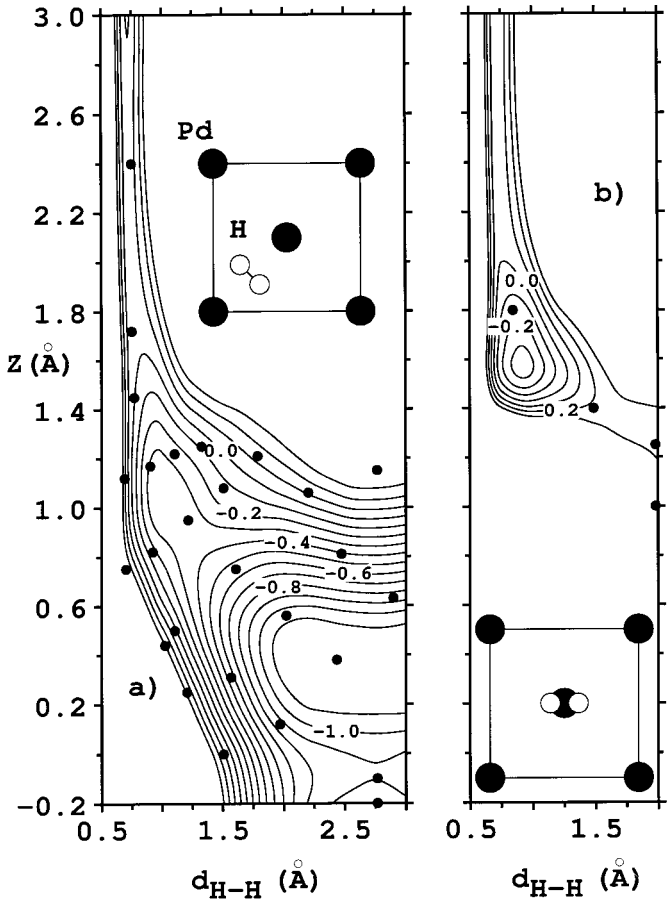

Fig. 5. Contour plots of the TB-PES along two two-dimensional cuts through the six-dimensional coordinate space of H_2/Pd (100), determined by a tight-binding Hamiltonian adjusted to ab initio calculations [34]. The notation corresponds to Fig. 2. The dots denote the points that have been used to obtain the fit. Energies are in eV per H_2 molecule. The contour spacing is 0.1 eV

to the fact that the quantum mechanical nature of bonding is taken into account properly by tight-binding methods [35], and that the parameters of the TBTE method, the Slater-Koster integrals [36], have a physical meaning, only a moderate number of input total energies is needed for a reliable global description of the PES.

The computational effort to determine total energies with a TBTE method is larger compared to an analytical representation since it requires the diagonalization of matrices. However, it is still much faster by about 2 to 3 orders of magnitude than ab initio total energy schemes. Either one can use the TB method directly to perform tight-binding molecular dynamics simulations, or one can use the information obtained by the TB total energies to adjust the parameters of a neural network which allows a fast evaluation of total energies, but needs at large number of input points for adjusting the parameters. In the first application of the TBTE method for the dissociation of hydrogen on Pd(100) [34] the tight-binding parameters describing the Pd–Pd interaction had been taken from an independent calculation [33, 37]. These parameters already reproduce Pd bulk and surface properties such as elastic constants and phonon energies. Hence this set of parameters can be used in simulations where the substrate atoms are no longer kept rigid but are treated as dynamical variables. This will allow to assess the influence of surface motion upon the hydrogen adsorption.

3.3 Performing ab initio dynamics simulations

The third step in the ab initio dynamics scheme involves the determination of the reaction dynamics. Once a reliable interpolation scheme is found, dynamics simulations can be carried out. Quantum mechanically this is done by plugging in the PES in a suitable form into the Hamiltonian and then solving either the time dependent [14] or the time-independent Schrödinger equation [38]. For solving the classical equation of motion, on the other hand, the gradient of the potential energy surface is needed, and then the equation of motion can be integrated numerically.

The first quantum dynamical treatment of hydrogen dissociation on surfaces in which all hydrogen degrees of freedom were treated dynamically was actually done by solving the time-independent Schrödinger equation in an efficient coupled-channel scheme. For details of the coupled-channel scheme we refer to Ref. [14].

Just recently this coupled-channel scheme has been implemented on a massively parallel computer, the Cray T3E. The code has been rewritten by using public domain libraries. However, the description of the dissociation in a time-independent method requires the use of curvelinear coordinates. Due to the use of curvelinear coordinates a non-symmetric matrix V has to be diagonalized which in the notation of Ref. [14] was denoted by q^2. Apparently, there are no massively parallel public domain diagonalisation schemes for general matrices available yet. For the particular problem of the molecular dissociation on surfaces we have therefore used a second order pertubation diagonalisation scheme which will be briefly sketched in the following. This schemes uses the fact that the anti-symmetric part of the matrix is small and can be treated as a pertubation.

First we decompose the matrix V_{nm} into a symmetric and an anti-symmetric part,

$$\begin{aligned} V_{nm} &= \frac{1}{2}(V_{nm} + V_{mn}) + \frac{1}{2}(V_{nm} - V_{mn}) \\ &\equiv V_{nm}^{\mathrm{sym}} + V_{nm}^{\mathrm{asym}} . \end{aligned} \tag{1}$$

The anti-symmetric part of the matrix which is related to the curvature of the curve-linear axis is in general sparse and small for the case of hydrogen dissociation on metal surfaces,

$$V_{nm}^{\text{asym}} \leq 0.1 V_{nm}^{\text{sym}} . \tag{2}$$

This allows to treat V^{asym} as a pertubation. First the symmetric part V^{sym} is diagonalised and the transformation matrix U determined. This matrix is used to transform V^{asym},

$$\tilde{V}^{\text{asym}} = U^{\text{T}} V^{\text{asym}} U . \tag{3}$$

The new eigenvalues are determined in a second order pertubation diagonalisation scheme via

$$E_n = \varepsilon_n + \sum_m{}' \frac{|\langle n|\tilde{V}^{\text{asym}}|m\rangle|^2}{\varepsilon_m - \varepsilon_n} . \tag{4}$$

Here the ε_m are the eigenvalues of the symmetric matrix. The prime denotes that the terms with $m = n$ are excluded from the sum.

Equivalently, the new eigenvectors are computed,

$$|N\rangle = |n\rangle + \sum_m{}' |m\rangle \frac{\langle m|\tilde{V}^{\text{asym}}|n\rangle}{\varepsilon_n - \varepsilon_m} + \sum_m{}' \sum_k{}' |m\rangle \frac{\langle m|\tilde{V}^{\text{asym}}|k\rangle\langle k|\tilde{V}^{\text{asym}}|n\rangle}{(\varepsilon_n - \varepsilon_k)(\varepsilon_n - \varepsilon_m)} . \tag{5}$$

This scheme assumes that the eigenvalues are non-degenerate. This requirement is fulfilled because $\tilde{V}^{\text{asym}}$ only couples different harmonic oscillator eigenstates which are always non-degenerate.

We have carefully checked the accuracy of this diagonalisation scheme. The error in the reaction probabilities due to the second order pertubation diagonalisation scheme is less than 0.5%. In Table 8 we have collected results concerning the performance of this second order diagonalisation scheme on a Cray T3E. This table shows that this scheme produces a reasonable speedup for up to 32 or 64 processors.

Figure 6 presents six-dimensional quantum dynamical calculations of the sticking probability using the coupled-channel method [14] as a function of the kinetic energy of a H_2 beam under normal incidence on a Pd(100) surface together with the integrated

Table 1
Performance of the massively parallel version of the coupled-channel quantum dynamics method [14] using a second order diagonalisation scheme on a Cray T3E

No. of PE	time (s)	speedup	MFlops/PE	total MFlops
1	4393	1.00	127	127
4	1035	4.24	132	530
16	282	15.60	124	1989
32	168	26.15	108	3464
64	109	40.30	80	5118
128	86	51.08	51	6487

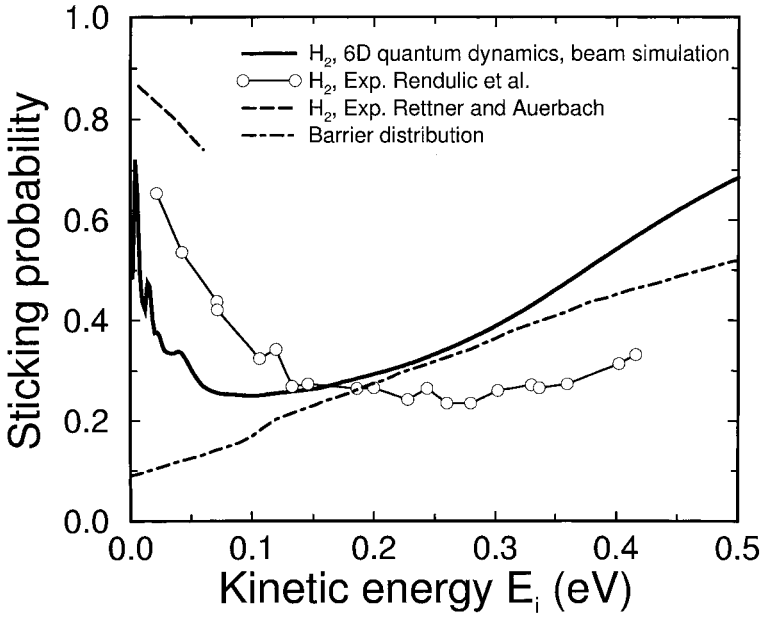

Fig. 6. Sticking probability versus kinetic energy for a hydrogen beam under normal incidence on a Pd(100) surface. Theory: six-dimensional results for H_2 molecules with an initial rotational and energy distribution adequate for molecular beam experiments (solid line) [11]; integrated barrier distribution: dash-dotted line. H_2 molecular beam adsorption experiment under normal incidence (Rendulic et al. [40]): circles; H_2 effusive beam scattering experiment with an incident angle of $\theta_i = 15°$ (Rettner and Auerbach [43]): long-dashed line

barrier distribution [10, 11]. The system H_2/Pd(100) is an experimentally well-studied system [39 to 43]. In Fig. 6 the results of H_2 molecular beam experiment by Rendulic et al. [40] and Rettner and Auerbach [43] are also plotted.

The integrated barrier distribution corresponds to the sticking probability in the classical sudden approximation or the so-called hole model [44]. Fig. 6 demonstrates that the static information gained from the barrier distribution is not sufficient in order to assess the reactivity of the H_2/Pd(100) system: At low kinetic energies the sticking probability is more than five times larger than what one would have estimated from the barrier distribution.

The high sticking probability at low kinetic energies, which agrees with the experiment, is caused by the steering effect: A slow molecule moving on a PES with non-activated as well as activated paths towards dissociation can be steered efficiently towards non-activated paths to adsorption by the forces acting upon the molecule even if the molecule approaches with an unfavorable initial configuration. This mechanism becomes less efficient at higher kinetic energies because then the molecule is too fast to be diverted significantly. Furthermore, Fig. 6 shows that at high kinetic energies the incoming molecules are still slightly steered since the sticking probability is larger than the integrated barrier distribution. However, in the intermediate range of $E_i \approx 0.25$ eV the sticking probability and the barrier distribution are rather close. At first sight this seems to be paradoxical. But a detailed analysis of swarms of classical trajectories on the same PES reveals that this behavior is caused by "negative" steering. Far away from

the surface the H_2 molecules are first steered towards the on top site. There they will eventually encounter a barrier (see Fig. 2b). At very low energies the molecules are then further steered to the bridge site, but at higher energies they are too fast, they hit the barrier at the top site and scatter back into the gas phase.

These results demonstrate the power or high-dimensional ab initio molecular dynamics calculations. Before this six-dimenensional study it was generally believed that a sticking probability decreasing with increasing kinetic energy is *always* caused by a precursor mechanism [40]. In this mechanism the molecules are assumed to be trapped molecularly in a precursor well before dissociation, and this trapping probability decreases with increasing kinetic energy. Now it is generally accepted that for hydrogen dissociation at reactive transition metal surfaces it is not necessary to invoke the precursor mechanism.

There is a dynamical property that allows to distinguish between steering and the precursor mechanism: the influence of the sticking probability on the rotational motion of the molecule. While steering is suppressed by additional rotational motion of the molecule [45], trapping in the molecular adsorption well in the presursor mechanism does not show any significant dependence on the initial rotational motion of the molecules [46].

Six-dimensional dynamical calculations have also been performed on the analytical representation of the ab initio PES of H_2 at $S(2 \times 2)$/Pd(100) in order to assess the dynamical consequences of the sulfur adsorption on the hydrogen dissociation [25]. The results of these quantum and classical calculations for the H_2 dissociative adsorption probability as a function of the incident energy are compared with experiment [39, 40] in Fig. 7.

First of all it is evident that the calculated sticking probabilities are significantly larger than the experimental results. Only the onset of dissociative adsorption at $E_i \approx 0.12$ eV is reproduced by the calculations. This onset is indeed also in agreement with the experimentally measured mean kinetic energy of hydrogen molecules desorbing from sulfur covered Pd(100) [39], which is denoted by the arrow in Fig. 7. We believe that those large differences between theory and experiment might be caused by the existence of subsurface sulfur which was, however, not discussed in the experimental studies. While the DFT calculations yield that the poisoning is caused by the building up of barriers hindering the dissociation, the vanishing hydrogen saturation coverage for roughly a quarter monolayer of adsorbed sulfur [42] suggests that any attractive adsorption sites for hydrogen have disappeared due to the presence of sulfur. These seemingly contradicting results and also the discrepancy between calculated and measured molecular beam sticking probabilities could be reconciled if subsurface sulfur plays an important role for the hydrogen adsorption energies. Subsurface sulfur is not considered in the calculations but might well be present in the experimental samples. The possible influence of subsurface species on reactions at surfaces certainly represents a very interesting and important research subject for future investigations.

Except for this open question, there are further interesting results obtained by the dynamical calculations. The calculated sticking probabilities are not only much larger than the experimental ones, they are also much larger than what one would expect from integrated barrier distribution, which corresponds to the sticking probability in the hole model [44]. This demonstrates that steering is not only operative for potential energy surfaces with non-activated reaction paths like for H_2/Pd(100), but also for activated systems as $H_2/S(2 \times 2)$/Pd(100). The huge corrugation of this system leads to an

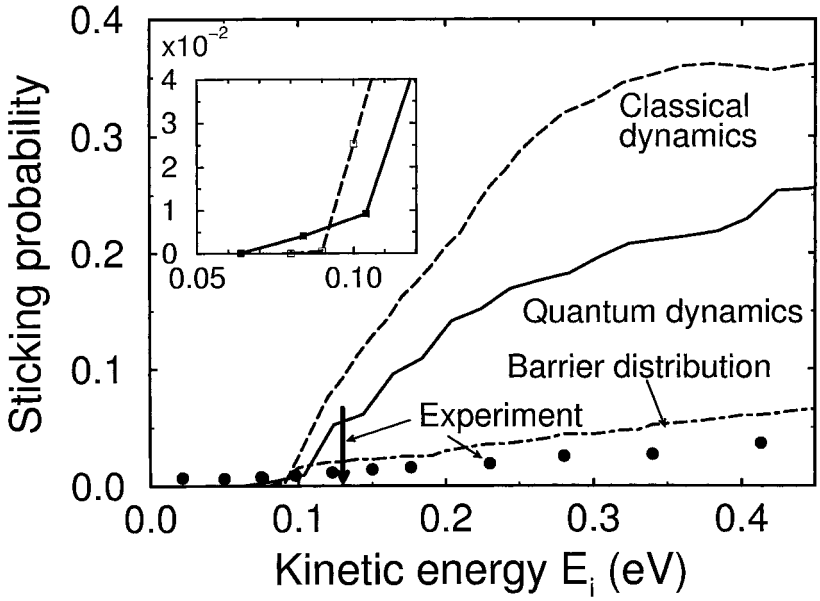

Fig. 7. Sticking probability versus kinetic energy for a H_2 beam under normal incidence on a $S(2 \times 2)$/Pd(100) surface. Full dots: experiment (from Ref. [40]); the arrow denotes the barrier towards adsorption deduced from desorption experiments [39]. Dashed-dotted line: integrated barrier distribution; solid line: quantum mechanical results for molecules initially in the rotational and vibrational ground-state; dashed line: classical results for initially non-rotating and non-vibrating molecules. The inset shows the quantum and classical results at low energies

enhancement of the sticking probability with respect to the hole model by a factor of three to four.

Figure 7 shows in addition that the classical molecular dynamics calculations overestimate the sticking probability of H_2 at $S(2 \times 2)$/Pd(100) compared to the quantum results. At small energies below the minimum barrier height the quantum calculations still show some dissociation due to tunneling, as the inset of Fig. 7 reveals, whereas the classical results are of course zero. But for higher energies the classical sticking probability is up to almost 50% larger than the quantum sticking probabilities. This suppression is also caused by the large corrugation and the anisotropy of the PES. The wave function describing the molecule has to pass narrow valleys in the PES in the angular and lateral degrees of freedom in order to dissociate. This leads to a localization of the wave function and thereby to the building up of zero-point energies which act as additional effective barriers. While the vibrational H–H mode becomes softer upon dissociation so that the zero-point energy in this particular mode decreases, for the system $H_2/S(2 \times 2)$/Pd(100) this decrease is over-compensated by the increase in the zero-point energies of the four other modes perpendicular to the reaction path, i.e., the sum of *all* zero-point energies increases upon adsorption [25]. Therefore the quantum particles experience an effectively higher barrier region causing the suppressed sticking probability compared to the classical particles. Interestingly enough, if the sum of all zero-point energies remains approximately constant along the reaction path as in the system H_2/Pd(100), then these quantum effects almost cancel out [10].

Furthermore, at energies slightly above the minimum energy barrier in Fig. 7, the quantum results are rather close to the classical results. This is caused by the fact that in this energy regime steering is much more efficient in the quantum than in the classical dynamics leading to a compensation of the hindering zero-point effects [47].

A final remark concerning the dynamical calculations: It is a common belief that classical trajectory calculations are less CPU-time consuming than quantum dynamical calculations. For the determination of a single trajectory this is certainly true, however, if it comes to the determination of reaction probabilities, then quantum methods can become more efficient. This is due to the fact that the evaluation of reaction probabilities requires averaging over initial conditions which is done automatically in quantum dynamics by choosing the appropriate initial quantum state. However, owing to the scaling properties with the number of atoms and the relative large memory requirement of quantum methods, one still has to rely on classical methods if dynamical simulations involving, say, more than ten degrees of freedom are to be performed.

4. Conclusions and Outlook

The last years have seen a tremendous step forward in the understanding of the interaction of molecules with surfaces. Based on advances in density functional theory algorithms, the potential energy surface of a molecule interacting with a surface can be mapped out in great detail. This development has motivated an increased effort in the dynamical simulation of processes on surfaces. The paradigm for simple reactions on surfaces – the dissociation of hydrogen on metal surfaces – seems to be understood to a large extent now, as this brief review has shown, although there are still open question. Consequently there is a lot of room for further investigations. In particular the importance of electronic transitions like electron–hole pair excitations upon adsorption is unknown yet. Currently also systems including oxygen – either in the substrate (oxide surfaces) or in the molecule (oxidation reactions) – are being addressed where electronic transitions are probably even more important.

The next great challenge is the description of more complex reactions and processes on surfaces. The study of these reactions is important not only for achieving one of the classical goals of surface science, which is a better understanding of heterogeneous catalysis. It is also directly relevant for a wide range of applications as the corrosion or passivation of surfaces, lubrication, growth properties for building better devices, the hydrogen storage in metals; and one even starts to address the microscopic description of biological systems. To investigate these reactions theoretically it is crucial not only to evaluate the potential energy surface on which the reaction takes place, but also to perform dynamical simulations on these potential energy surfaces to actually obtain reaction rates and probabilities. Since in many problems surface processes occur on a long time scale and/or on a large length scale, also appropriate statistical and analytical methods to deal with these different scales have to be developed and applied. The theoretical treatment of reactions on surfaces is certainly a growing research field.

Acknowledgements It is a pleasure to acknowledge the co-workers who have made this work possible. I like to thank Michel Bockstedte, Wilhelm Brenig, Mike Mehl, Dimitri Papaconstantopoulos, Matthias Scheffler, Ching-Ming Wei and Steffen Wilke. Special thanks go to Jakob Pichlmeier for creating the massively parallel version of the coupled-channel scheme.

References

[1] A. Gross, Surf. Sci. Rep. **32**, 291 (1998).
[2] B. Hammer, M. Scheffler, K.W. Jacobsen, and J.K. Nørskov, Phys. Rev. Lett. **73**, 1400 (1994).
[3] J.A. White, D.M. Bird, M.C. Payne, and I. Stich, Phys. Rev. Lett. **73**, 1404 (1994).
[4] S. Wilke and M. Scheffler, Phys. Rev. B **53**, 4296 (1996).
[5] A. Eichler, G. Kresse, and J. Hafner, Phys. Rev. Lett. **77**, 1119 (1996).
[6] C. Stampfl and M. Scheffler, Phys. Rev. Lett. **78**, 1500 (1997).
[7] A. Eichler, J. Hafner, A. Gross, and M Scheffler, Phys. Rev. B **59**, 13297 (1999).
[8] A. De Vita, I. Štich, M.J. Gillan, M.C. Payne, and L.J. Clarke, Phys. Rev. Lett. **71**, 1276 (1993).
[9] A. Gross, M. Bockstedte, and M. Scheffler, Phys. Rev. Lett. **79**, 701 (1997).
[10] A. Gross and M. Scheffler, Phys. Rev. B **57**, 2493 (1998).
[11] A. Gross, S. Wilke, and M. Scheffler, Phys. Rev. Lett. **75**, 2718 (1995).
[12] M. Kay, G.R. Darling, S. Holloway, J.A. White, and D.M. Bird, Chem. Phys. Lett. **245**, 311 (1995).
[13] G.J. Kroes, E.J. Baerends, and R.C. Mowrey, Phys. Rev. Lett. **78**, 3583 (1997).
[14] W. Brenig, T. Brunner, A. Groß, and R. Russ, Z. Phys. B **93**, 91 (1993).
[15] K.W. Kolasinski, Internat. J. Mod. Phys. B **9**, 2753 (1995).
[16] K.W. Kolasinski, W. Nessler, A. de Meijere, and E. Hasselbrink, Phys. Rev. Lett. **72**, 1356 (1994).
[17] K.W. Kolasinski, W. Nessler, K.-H. Bornscheuer, and E. Hasselbrink, J. Chem. Phys. **101**, 7082 (1994).
[18] P. Bratu, W. Brenig, A. Gross, M. Hartmann, U. Höfer, P. Kratzer, and R. Russ, Phys. Rev. B **54**, 5978 (1996).
[19] A.J.R. da Silva, M.R. Radeke, and E.A. Carter, Surf. Sci. **381**, L628 (1997).
[20] M. Bockstedte, A. Kley, J. Neugebauer, and M. Scheffler, Comput. Phys. Commun. **107**, 187 (1997).
[21] A. Eichler, G. Kresse, and J. Hafner, Surf. Sci. **397**, 116 (1998).
[22] C.M. Wei, A. Gross, and M. Scheffler, Phys. Rev. B **57**, 15572 (1998).
[23] B. Hammer and M. Scheffler, Phys. Rev. Lett. **74**, 3487 (1995).
[24] S. Wilke and M. Scheffler, Phys. Rev. Lett. **76**, 3380 (1996).
[25] A. Gross, C.M. Wei, and M. Scheffler, Surf. Sci. **416**, L1095 (1998).
[26] G. Wiesenekker, G.J. Kroes, and E.J. Baerends, J. Chem. Phys. **104**, 7344 (1996).
[27] G.J. Kroes, E.J. Baerends, and R.C. Mowrey, J. Chem. Phys. **110**, 2738 (1999).
[28] T.B. Blank, S.D. Brown, A.W. Calhoun, and D.J. Doren, J. Chem. Phys. **103**, 4129 (1995).
[29] K.T. No, B.H. Chang, S.Y. Kim, M.S. Jhon, and H.A. Scheraga, Chem. Phys. Lett. **271**, 152 (1997).
[30] S. Lorenz, A. Gross, and M. Scheffler, APS Bull. **43**, 235 (1998).
[31] D.E. Makarov and H. Metiu, J. Chem. Phys. **108**, 590 (1998).
[32] R.E. Cohen, M.J. Mehl, and D.A. Papaconstantopoulos, Phys. Rev. B **50**, 14694 (1994).
[33] M.J. Mehl and D.A. Papaconstantopoulos, Phys. Rev. B **54**, 4519 (1996).
[34] A. Gross, M. Scheffler, M.J. Mehl, and D.A. Papaconstantopoulos, Phys. Rev. Lett. **82**, 1209 (1999).
[35] G.M. Goringe, D.R. Bowler, and E. Hernández, Rep. Progr. Phys. **60**, 1447 (1997).
[36] J.C. Slater and G.F. Koster, Phys. Rev. **94**, 1948 (1954).
[37] WWW address: http://cst-www.nrl.navy.mil/bind
[38] G.R. Darling and S. Holloway, Rep. Progr. Phys. **58**, 1595 (1995).
[39] G. Comsa, R. David, and B.-J. Schumacher, Surf. Sci. **95**, L210 (1980).
[40] K. D. Rendulic, G. Anger, and A. Winkler, Surf. Sci. **208**, 404 (1989).
[41] L. Schröter, H. Zacharias, and R. David, Phys. Rev. Lett. **62**, 571 (1989); Surf. Sci. **258**, 259 (1991).
[42] M.L. Burke and R.J. Madix, Surf. Sci. **237**, 1 (1990).
[43] C.T. Rettner and D.J. Auerbach, Chem. Phys. Lett. **253**, 236 (1996).
[44] M. Karikorpi, S. Holloway, N. Henriksen, and J.K. Nørskov, Surf. Sci. **179**, L41 (1987).
[45] A. Gross, S. Wilke, and M. Scheffler, Surf. Sci. **357/358**, 614 (1996).
[46] M. Beutl, K.D. Rendulic, and G.R Castro, Surf. Sci. **385**, 97 (1997).
[47] A. Gross, J. Chem. Phys. **110**, 8696 (1999).